Proceedings of the 9th International Conference on Fluid Flow, Heat and Mass Transfer (FFHMT'22)
Niagara Falls, Canada – June 08-10, 2022
Paper No. 125
DOI: 10.11159/ffhmt22.125

Influence of Porous Oxide Layer on Water Spray Cooling

Ondřej Resl[1], Martin Chabičovský[1], Milan Hnízdil[1], Petr Kotrbáček[1], Miroslav Raudenský[1]
[1]Brno University of Technology, Faculty of Mechanical Engineering
Technická 2896/2, 616 69, Brno, Czech Republic
Ondrej.Resl@vut.cz; Martin.Chabicovsky@vut.cz; Milan.Hnizdil@vut.cz; Petr.Kotrbacek@vut.cz;
Miroslav.Raudensky@vut.cz

Abstract - Steel production and processing are connected with the formation of an oxide layer on a hot surface of steel. The oxide layer influences cooling and the final quality of the steel. Spray cooling is mainly influenced by water impingement density and by surface temperature, but the influence of the oxide layer is not negligible. The oxide layer can be considerably porous. The porosity of the oxide layer significantly influences its thermal conductivity, because air pores have much lower thermal conductivity compared to pure oxides. In this paper, the influence of the oxide layer on water spray cooling is experimentally and numerically investigated. The heat transfer coefficient of an oxidized steel surface and a clean steel surface are compared and the effect of the oxide layer on the Leidenfrost temperature is studied. Also, the porosity of the oxide layer and the average thermal conductivity of the porous oxide layer are determined for different oxidation regimes.

***Keywords*:** Oxides, scales, spray cooling, heat transfer coefficient, Leidenfrost temperature, porosity, thermal conductivity

1. Introduction

Water spray cooling is a common way of cooling in many fields of human activity. It is used for example in healthcare or for electronics cooling, but mainly in the steel industry. Due to high temperatures during steel production and processing, oxides form on the hot steel surface. The layer of oxides consists of various oxides (FeO, Fe_3O_4, Fe_2O_3 etc.) and its thickness and structure are influenced by the chemical composition of steel, the temperature and the surrounding atmosphere during oxidation.

The oxide layer has an influence on the cooling of the steel and affects the final properties and quality of the steel [1, 2]. Spray cooling depends on many parameters [3]. The influence of the oxide layer on spray cooling is not as significant as, for example, water impingement density or surface temperature, but is not negligible, so it should be studied. The oxide layer can be very porous. Air pores have much lower thermal conductivity than pure oxides and, due to this fact, the porosity of the oxide layer has a significant influence on the thermal conductivity of the whole oxide layer. The thermal conductivity of the porous oxide layer is very low compared to the steel and this layer acts as an insulant. Furthermore, the oxide layer can increase the Leidenfrost temperature (temperature corresponding to the minimal heat flux) and influence the cooling intensity and homogeneity [4]. In addition, the surface roughness of the steel is changed after oxidation [5], which can lead to a change in cooling [6].

Knowledge of the thermophysical properties of the porous oxide layer is necessary for a numerical simulation of the spray cooling. The main parameters which influence heat transfer through the porous oxide layer are the thickness and thermal conductivity of this layer. The thermal conductivity of the pure oxides which occur in the oxide layer (typically wüstit, magnetit or hematite) can easily be found in literature [7, 8, 9], but porosity is not taken into consideration. The thermal conductivity of the whole oxide layer is not frequently reported. In [10] the thermal conductivity of the oxide layer created by oxidation on low carbon steel can be found. Thermal conductivity is determined for room temperature, but there is no information about porosity. The thermal conductivity of the porous oxide layer with information about its porosity can be found in [11].

This paper builds on previously published articles [4, 12] and develops them. The influence of the oxide layer on water spray cooling is studied. The effect of the oxide layer on the Leidenfrost temperature and heat transfer coefficient is experimentally and numerically investigated and the average thermal conductivity of the porous oxide layer is determined by FEM modelling for different oxidation regimes.

2. Porosity of the oxide layer

2.1. Oxidation of steel samples

Samples of 20x20x25 mm from 54SiCr6 steel were prepared to determine the porosity of the oxide layer. The samples were oxidized in different oxidation regimes (Table 1). The oxidation time was between 15 and 60 minutes and the temperature of oxidation was 900 °C and 1050 °C.

Table 1: The oxidation regimes.

Temperature of oxidation [°C]	Oxidation time [min]		
	15	30	60
900	A1	A2	A3
1050	B1	B2	

Two samples were oxidized in each regime and two representative parts from the oxidized surface of each sample were chosen for observation under an optical microscope after oxidation.

2.2. Analysis of the porosity of the oxide layer

The porosity of the oxide layer was determined by using pictures from the optical microscope as is described in [12, 13]. A picture of the oxide layer with its histograms of R (red), G (green) and B (blue) values of the RGB space is in Fig. 1. The dark layer at the top of Fig. 1 represents a fixing glue which was used during sample preparation for microscope observation. In the middle there are oxides with air pores (dark areas) and at the bottom there is steel (light layer). We can see that the histograms are bimodal. Areas “A” (in the histograms in Fig. 1) represent the fixing glue and air pores, areas “B” represent oxides and areas “C” represent steel. Based on this information, the oxide layer was segmented by thresholding and the porosity of the oxide layer was calculated from a picture of the segmented oxide layer and a picture of the segmented oxide layer with filled air pores.

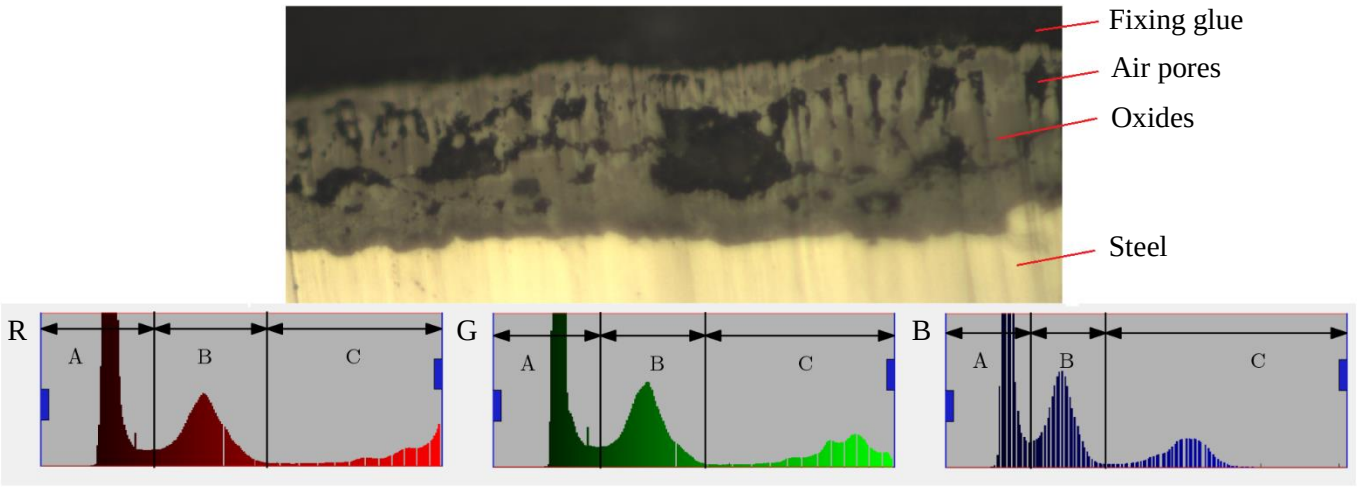

Fig. 1: Picture of the oxide layer with its histograms.

The values of the average porosity of the oxide layer and their standard deviation are for each oxidation regime in Table 2. (Four parts of the samples were used to determine the average porosity in each oxidation regime). It can be seen that the average porosity increases with the temperature of oxidation (the oxidation temperature was 900 °C for regimes A and 1050 °C for regimes B). It is also evident that longer oxidation time causes higher average porosity for oxidation regimes A. This is not observed in oxidation regimes B, but information about longer oxidation times is

missing. Based on previous research and literature [13], an increase in porosity for longer oxidation times can be also expected.

Table 2: Porosity of the oxide layer for different oxidation regimes.

Regime of oxidation	A1	A2	A3	B1	B2
Porosity [%]	19.3	24.1	44.6	29.4	29.1
Standard deviation [%]	6.2	11.5	13.7	7.9	8.0

3. Thermal conductivity of the porous oxide layer

The information about the porosity of the oxide layer was used for the determination of the average thermal conductivity of the porous oxide layer. The representative part of sample was chosen based on analysis of oxide layer porosity for every oxidation regime and pictures of these parts from the optical microscope were redrawn in AutoCAD. Next, the redrawn pictures were used as a 2D input geometry for calculation of the average thermal conductivity of the porous oxide layer. The boundary conditions T_p and T_s (Fig. 2) were chosen so that the value of temperature T_p was always five degrees lower than the temperature at which the average thermal conductivity of the porous oxide layer was determined and the value of temperature T_s was always five degrees higher. The result of steady-state thermal analysis conducted in ANSYS Workbench was the position-dependent heat flux on the boundary with temperature T_s, which was subsequently integrated and divided by the length of the boundary with temperature T_s. Next, the average thermal conductivity of the porous oxide layer was calculated from the Eq. (1).

$$\bar{k} = \frac{q''\delta}{(T_s - T_p)} \tag{1}$$

The $\bar{k}$ in Eq. (1) is the average thermal conductivity of the porous oxide layer, q'' is the heat flux and δ is the thickness of the oxide layer that was determined from pictures from the optical microscope. The FeO oxide was considered in the case of oxidation regimes A1-A3. In the case of oxidation regimes B1 and B2, the FeO and Fe_3O_4 oxides were considered, but the Fe_3O_4 oxide was only found in a thin layer near the steel surface. Oxides FeO and Fe_3O_4 were chosen based on the diagram in [14].

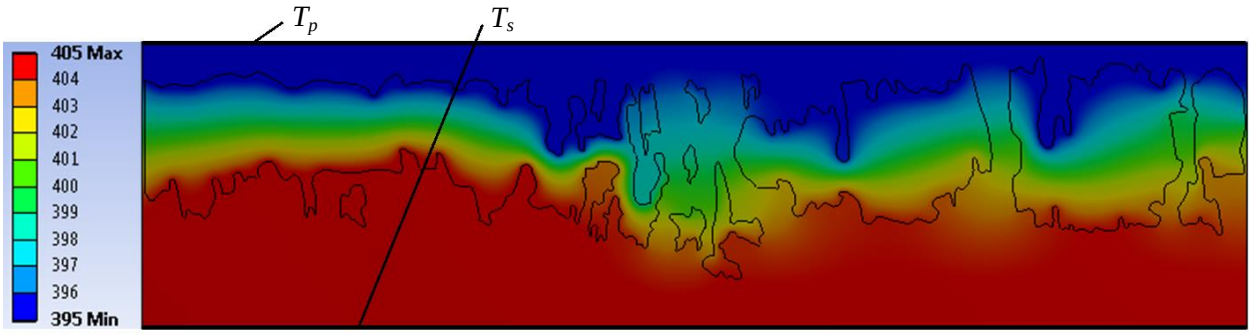

Fig. 2: Temperature distribution of the porous oxide layer.

The average thermal conductivity of the porous oxide layer dependent on the temperature for different oxidation regimes is in Fig. 3. The porosity of the chosen parts of the samples was 21.7 % for oxidation regime A1, 27.6 % for A2, 45 % for A3, 30.7 % for B1 and 28.7 % for B2. The oxide layer without air pores (with zero porosity) is also added to Fig. 3 (black line) and thus the significant influence of the porosity on the average thermal conductivity is evident.

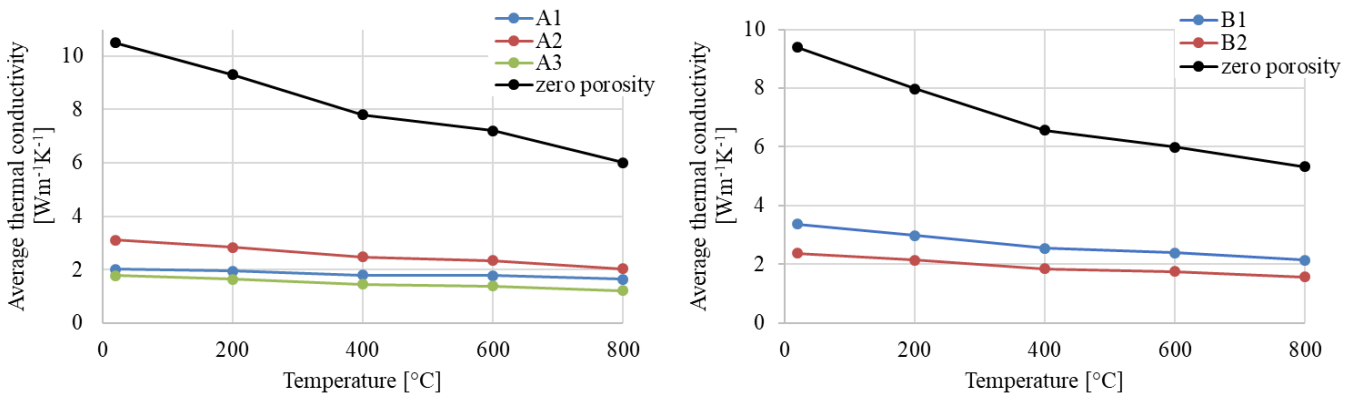

Fig. 3: The average thermal conductivity dependent on the temperature.

The value of thermal conductivity of the oxide layer $k = 3.8$ $Wm^{-1}K^{-1}$ can be found in [10]. This thermal conductivity is determined for room temperature, but the porosity of the oxide layer is not mentioned. The value of thermal conductivity of the porous oxide layer $k = 1.2$ $Wm^{-1}K^{-1}$ is determined for temperature $T = 800$ °C and porosity 37 % in [11]. Higher values of thermal conductivity were observed in comparison to the results from [11].

The average thermal conductivity of the oxide layer dependent on the porosity of the oxide layer is in Fig 4. From this figure it can be seen that the average thermal conductivity of the porous oxide layer does not have to decrease as porosity grows. For example, if we compare the samples oxidized in regime A1 and A2 (with porosity of 21.7 % and 27.6 % respectively), the average thermal conductivity is higher for the oxide layer with greater porosity. This phenomenon can be explained by the distribution of air pores. Air pores formed a continuous thin layer across almost the whole picture in the case of the sample oxidized in regime A1 (Fig. 5a). Nothing similar was observed for the sample oxidized in regime A2 (Fig, 5b). The same situation occurred in the case of the samples oxidized in regimes B1 and B2. Therefore, the distribution of air pores can significantly influence the average thermal conductivity of the porous oxide layer.

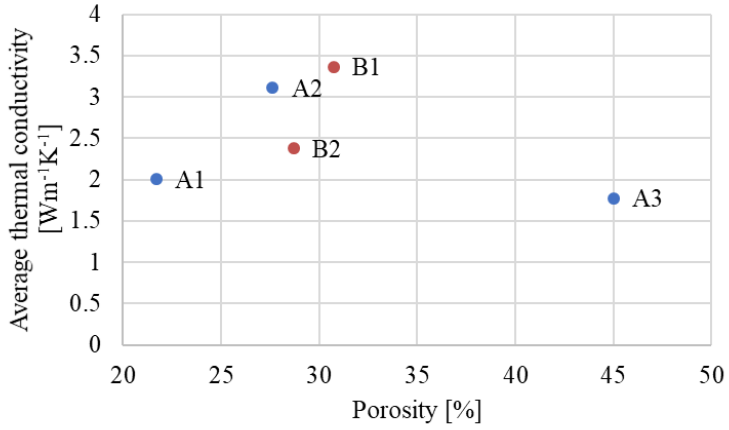

Fig. 4: The average thermal conductivity dependent on the porosity of the oxide layer.

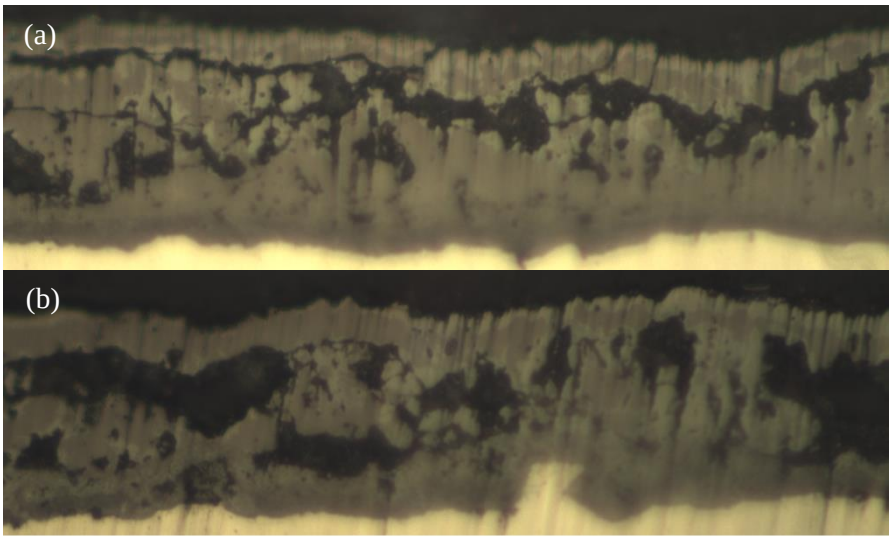

Fig. 5: Distribution of air pores for oxidation regime A1 (a) and A2 (b).

4. Influence of the oxide layer on water spray cooling

4.1. Heat transfer coefficient measurement

Samples of 155x60x25 mm from 54SiCr6 steel were used for heat transfer coefficient (HTC) measurement. One sample did not have an oxide layer and one sample was oxidized at a temperature of 900 °C for 60 minutes (oxidation regime A3). Each sample was equipped with two shielded grounded thermocouples (type K). The thermocouples were placed into holes drilled 2 mm from the cooled surface (Fig. 6).

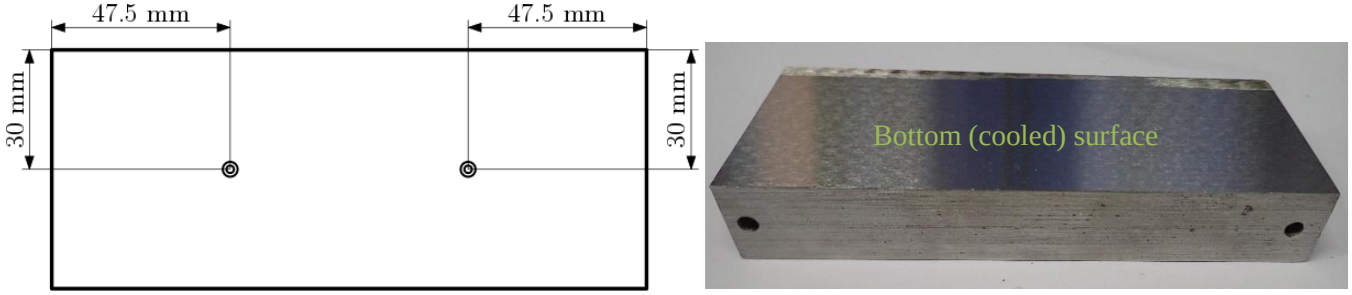

Fig. 6: Test sample and position of holes for thermocouples.

After the thermocouples were set into position, the sample was isolated from the top side (the bottom side was cooled), placed in a furnace and heated to 760 °C. A protective atmosphere was used to avoid additional oxidation. The sample was placed on the test bench (Fig. 7) after the required temperature was achieved. Then the cooling started.

The flat jet nozzle (SS.CO 8006) with a spray angle of 80° was used for the cooling. The distance between the nozzle and the cooled surface was 300 mm and the nozzle was placed under the centre of the sample. The water pressure was 2 bar and the flow rate was 0.114 m^3h^{-1}.

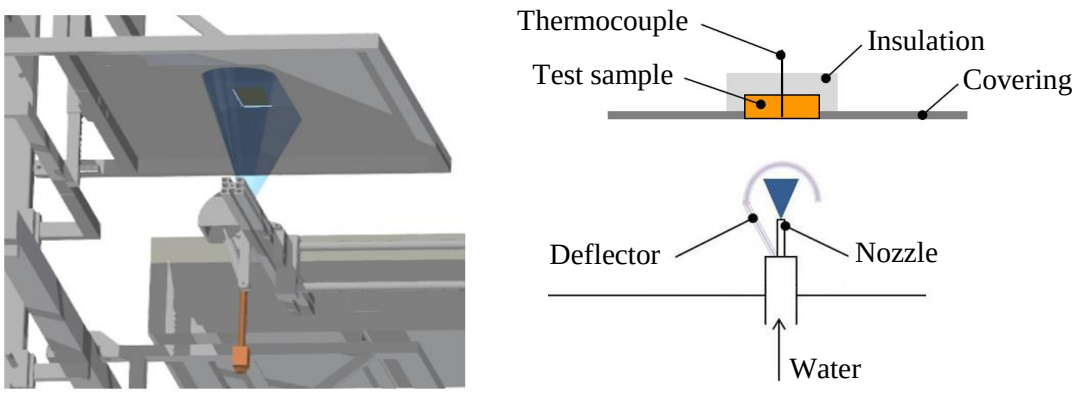

Fig. 7: Test bench.

4.2. Results

The inverse heat conduction problem was used to compute the time-dependent boundary conditions (heat flux, surface temperature, HTC), because the temperatures were measured 2 mm under the steel surface. Beck's sequential method was applied [15] and the dependence of the HTC and heat flux on the surface temperature were obtained directly. The HTC and heat flux dependent on surface temperature are shown in Fig. 8. The average values from the pair of thermocouples were used for both surfaces (clean and oxidized).

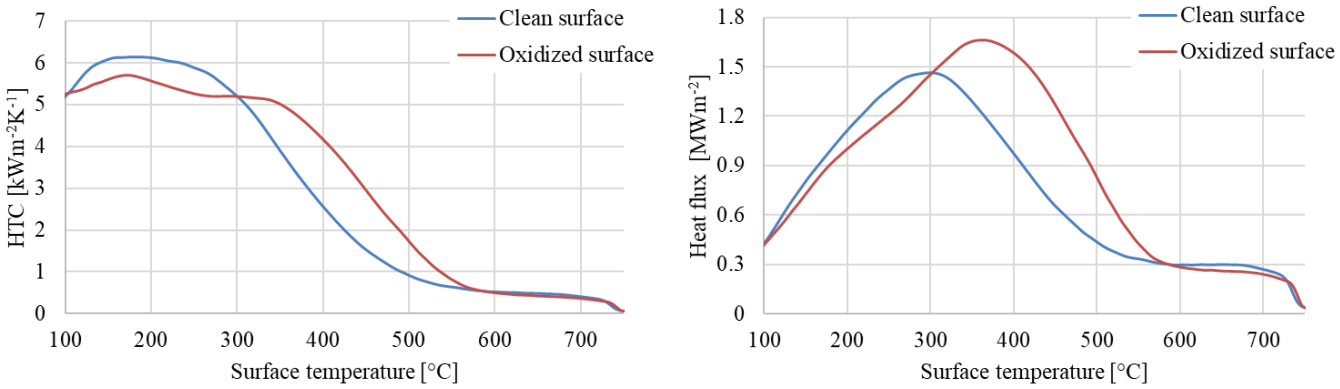

Fig. 8: HTC and heat flux for clean and oxidized surface.

As can be seen, the HTC of oxidized surface is a little lower in high temperature region (temperature higher than approximately 580 °C) and also for temperatures lower than 300 °C. It is caused by low thermal conductivity of the oxide layer in comparison with thermal conductivity of steel. Different situation occurs for surface temperatures between 300 °C and 580 °C. The HTC of oxidized surface is higher in this temperature range. This is caused by the change in the Leidenfrost temperature. The Leidenfrost temperature is a temperature corresponding to the minimal heat flux as was mentioned before. From Fig. 8 is evident that the oxide layer increases the Leidenfrost temperature. The Leidenfrost temperature is around 600 °C for clean surface and 640 °C for oxidized surface.

5. Numerical simulation

The 1D numerical simulation of the influence of the oxide layer on water spray cooling was conducted based on the information obtained about the average thermal conductivity of the porous oxide layer. The data measured from

one thermocouple was used for the simulation and the oxide layer directly above the thermocouple was observed. The thickness of the oxide layer was 130 µm. The model used is shown in Fig. 9a.

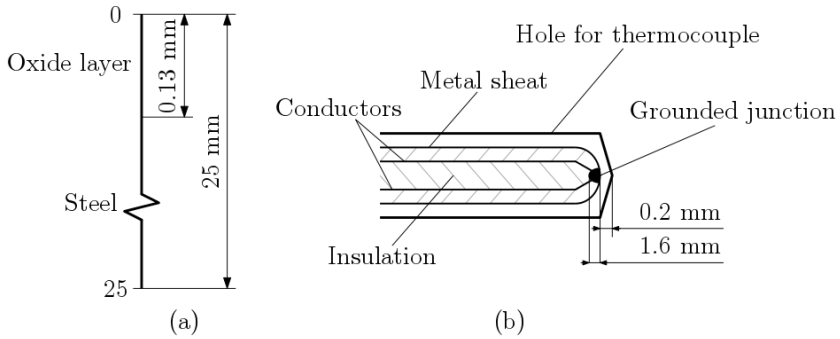

Fig. 9: The model of numerical simulation (a) and thermocouple description (b).

The thickness of the oxide layer was 0.13 mm, the hole for the thermocouple was 1.97 mm from the clean surface, the thickness of the junction was 1.6 mm and the space between the thermocouple and the steel was 0.2 mm (Fig. 9b). This information shows that the data was recorded 3.9 mm under the oxidized surface. The model does not include the thermocouple.

Thermal conductivity from Fig. 3 (regime A3) was used. The HTC of the clean surface (average from two thermocouples) was used as a boundary condition. This boundary condition was then modified by the surface roughness, because the surface roughness of the steel changed after oxidation [5]. The modification was done by interpolation between the surface roughness of the grinded and rolled surface. The temperature of the water was 19.4 °C during spray cooling and the initial temperature of the sample was 757 °C.

Conducted simulations and data from measurement are in Fig. 10. Simulation without oxide layer (Sim.: clean surface) was also conducted. From Fig. 10 it can be seen that numerical simulation with boundary condition without modification (Sim.: ox. surface) differs from measurement. The numerical simulation with modified boundary condition (Sim.: ox. surface, modified) models experiment pretty well in the high temperature area and also in the area around Leidenfrost temperature. Numerical simulations also confirmed the increase of Leidenfrost temperature and insulation effect of the oxide layer.

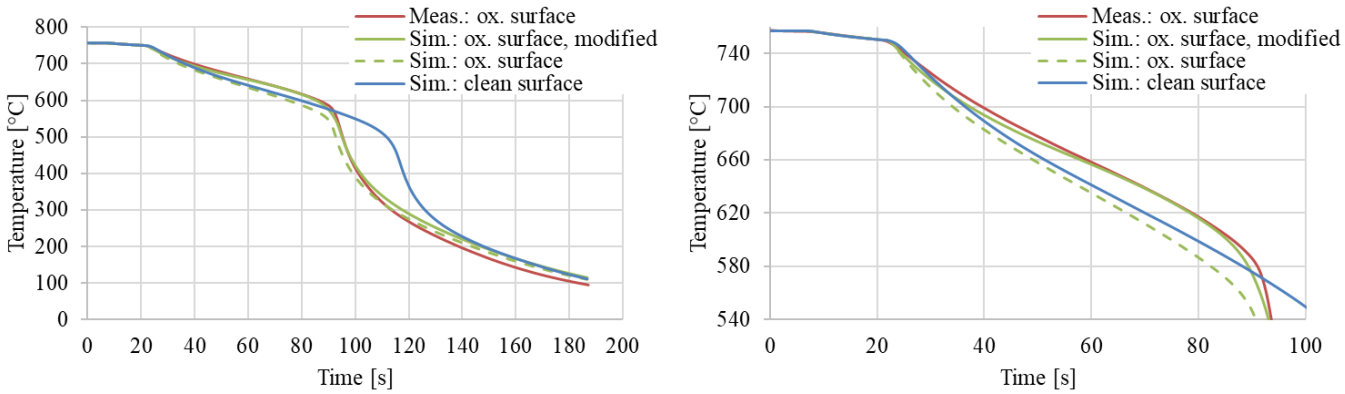

Fig. 10: Conducted simulations and data from measurement (left graph: all data; right graph: detail of the high temperature area).

6. Conclusion

The porosity of the oxide layer was studied and the average thermal conductivity of the porous oxide layer was determined for different oxidation regimes. It was found that the porosity of the oxide layer increases with time and

temperature of oxidation and the average thermal conductivity of the porous oxide layer is significantly influenced not only by the porosity of the oxide layer but also by the distribution of air pores. If air pores form a continuous thin layer over a large area, the average thermal conductivity of this oxide layer can be lower than in the case of an oxide layer with higher porosity and no continuous thin layer of air pores.

Also, the effect of the oxide layer on the HTC and the Leidenfrost temperature during water spray cooling was investigated experimentally. It was shown that the oxide layer acts like thermal barrier (in a high temperature region) and increases the Leidenfrost temperature. The difference between the Leidenfrost temperature of the sample with a clean surface and the Leidenfrost temperature of the sample with an oxidized surface was around 40 °C. These results were confirmed by conducting a numerical simulation.

Acknowledgements

The research leading to these results has received funding from the Ministry of Education, Youth and Sports under the programme INTER _ EXCELLENCE, within the project LTAUSA19053.

References

[1] R. Wendelstorf, K. -H. Spitzer, and J. Wendelstorf, "Effect of oxide layers on spray water cooling heat transfer at high surface temperatures", *International Journal of Heat and Mass Transfer*, vol. 51, pp. 4892-4901, 2008.

[2] M. Chabičovský, M. Hnízdil, A. A. Tseng, and M. Raudenský, "Effects of oxide layer on Leidenfrost temperature during spray cooling of steel at high temperatures", *International Journal of Heat and Mass Transfer*, vol. 88, pp. 236–246, 2015.

[3] G. Liang and I. Mudawar, "Review of spray cooling - Part 1: Single-phase and nucleate boiling regimes, and critical heat flux", *International Journal of Heat and Mass Transfer*, vol. 115, pp. 1174-1205, 2017.

[4] M. Chabičovský, O. Resl, and M. Raudenský, "Impact of oxide layer on spray cooling intensity and homogeneity during continuous casting of the steel", in *METAL 2018, 27rd International Conference on Metallurgy and Materials, Conference Proceedings*, 2018, pp. 69-74.

[5] W. Sun, A. K. Tieu, Z. Jiang, H. Zhu, and C. Lu, "Oxide scales growth of low-carbon steel at high temperatures", *Journal of Materials Processing Technology*, vol. 155-156, pp. 1300-1306, 2004.

[6] H. Fukuda, N. Nakata, H. Kijima, T. Kuroki, A. Fujibayashi, Y. Takata, and S. Hidaka, "Effects of Surface Conditions on Spray Cooling Characteristics", *ISIJ International*, vol. 56, no. 4, pp. 628–636, 2016.

[7] R. Colás, "Modelling heat transfer during hot rolling of steel strip", *Modelling and Simulation in Materials Science and Engineering*, vol. 3, no. 4, pp. 437-453, 1995.

[8] D. Genève, D. Rouxel, P. Pígeat, and M. Confente, "Descaling ability of low-alloy steel wires depending on composition and rolling process", *Corrosion Science*, vol. 52, no. 4, pp. 1155-1166, 2010.

[9] M. Takeda, T. Onishi, S. Nakakubo, and S. Fujimoto, "Physical Properties of Iron-Oxide Scales on Si-Containing Steels at High Temperature", *Materials Transactions*, vol. 50, no. 9, pp. 2242-2246, 2009.

[10] R. Endo, T. Yagi, M. Ueda, and M. Susa, "Thermal Diffusivity Measurement of Oxide Scale Formed on Steel during Hot-rolling Process", *ISIJ International*, vol. 54, no. 9, pp. 2084-2088, 2014.

[11] M. Pohanka, M. Chabičovský, and T. Ondruch, "Thermophysical properties measurement of scale layer on steel substrate using flash method", in *24th international conference on materialsand technology*, 2016, pp. 175-175.

[12] O. Resl, M. Chabičovský, and H. Votavová, "Study of thermal conductivity of the porous oxide layer", in *Eegineering Mechanics 2019, 25th International Conference*, 2019, pp. 315-318.

[13] O. Resl, "Vliv vrstvy oxidů na chlazení ocelových povrchů", Master's thesis, Fakulta strojního inženýrství, Vysoké učení technické v Brně, Brno, 2018. Available: https://www.vutbr.cz/www_base/zav_prace_soubor_verejne.php?file_id=173687

[14] D. T. Blazevic, Hot strip mill operations. Sun Lakes, Ariz.: D.T. Blazevic, 2011.

[15] J. V. Beck, B. Blackwell, and R. C. Charles, *Inverse heat conduction: ill-posed problems*. New York: Wiley, c1985.